catalysts

MDPI

*Article*

# Supplementary Materials Point-defect-rich carbon sheets as the high-activity catalyst toward oxygen reduction and hydrogen evolution

**Wenjing Yuan †, Fuhua Zhang †, Yaoyao Wu , Xiaotao Chen , Chihhsiang Fang and Chuanhao Li ***

Guangdong Provincial Key Laboratory of Environmental Pollution Control and Remediation Technology, School of Environmental Science and Engineering, Sun Yat-sen University, Guangzhou 510006, PR China; yuanwj7@mail.sysu.edu.cn; zhangfh5@mail2.sysu.edu.cn; wuyy69@mail2.sysu.edu.cn; chenxt68@mail2.sysu.edu.cn; fangch29@mail2.sysu.edu.cn

* Correspondence: lichuanh3@mail.sysu.edu.cn

† These authors contributed equally to this work.

## 1. Formation mechanism of graphene-like mesoporous carbon sheets

The formation mechanism of graphene-like mesoporous carbon sheets are illustrated in Scheme 1. Calcium gluconate is encapsulated by ethanol, which is decomposed easily in situ production a lot of $CO_2$ via burning ethanol, and these $CO_2$-bubbles play a key role for the formation of graphene-like mesoporous carbon sheets. At this point, calcium gluconate will change from solid state to molten state. A large number $CO_2$-bubbles was formed at different locations in the interior of precursor, which build a series of channels by extrusion process from the interior to precursor-air interface. Where there are $CO_2$-bubbles, there will be no carbon precursor. Therefore, the carbon precursor is only existed in the gaps of $CO_2$-bubbles, resulting in the formation of graphene-like mesoporous carbon sheets.

## 2. Electron transfer number and $H_2O_2$ yield

The electrocatalytic oxygen reduction reaction pathway of sample was evaluated by RRDE measurement. The electron transfer number ($n$) and $H_2O_2$ yield can be calculated from the following the Eq. (1) and Eq. (2):

$$n = 4 \times \frac{I_D}{I_D + I_R / N} \quad (1)$$

$$H_2O_2(\%) = 200 \times \frac{I_R/N}{I_D + I_R/N} \quad (2)$$

Here, $I_D$, $I_R$ and $N$ are the disk current, ring current and collection efficiency of the Pt ring, respectively [1].

## 3. RHE Calibration

All potentials were converted to the reversible hydrogen electrode (RHE) scale based on the Nernst equation [2]:

$$E_{RHE} = E_{Ag/AgCl} + 0.2046\ V + 0.059\,pH \quad (3)$$

## 4. Tafel plot

Tafel slopes were calculated by fitting the linear portions of Tafel plots to the Tafel equation[3]:

$$\eta = b \log J + a \quad (4)$$

Where, $\eta$, $b$, $J$ and $a$ are the overpotential, Tafel slope, current density, and empirical coefficient.

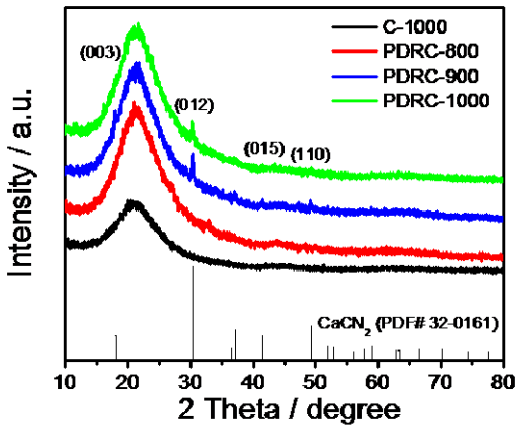


**Figure S1.** XRD patterns of C-1000, PDRC-800, PDRC-900 and PDRC-1000.

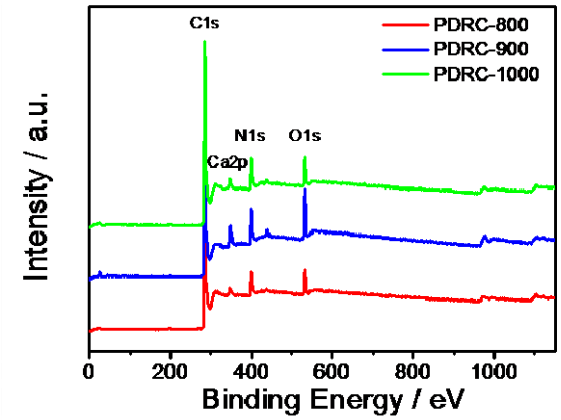


**Figure S2.** XPS data of PDRC-800, PDRC-900 and PDRC-1000.

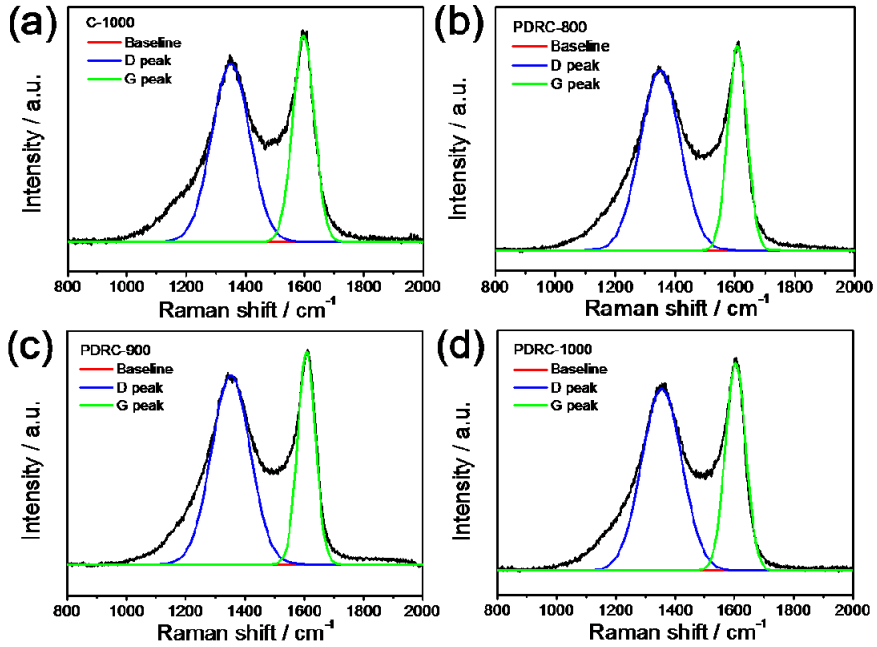


**Figure S3.** Raman spectra of (a) C-1000, (b) PDRC-800, (c) PDRC-900 and (d) PDRC-1000.

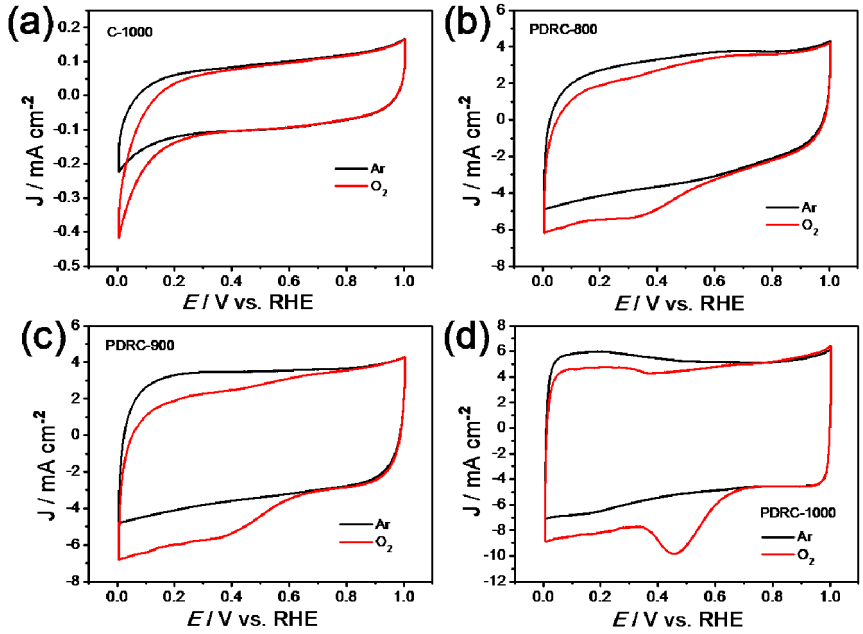


**Figure S4.** CV curves of (a) C-1000, (b) PDRC-800, (c) PDRC-900 and (d) PDRC-1000 (scan rate 150 mV $s^{-1}$) in Ar- or $O_2$-saturated 0.5 M $H_2SO_4$.

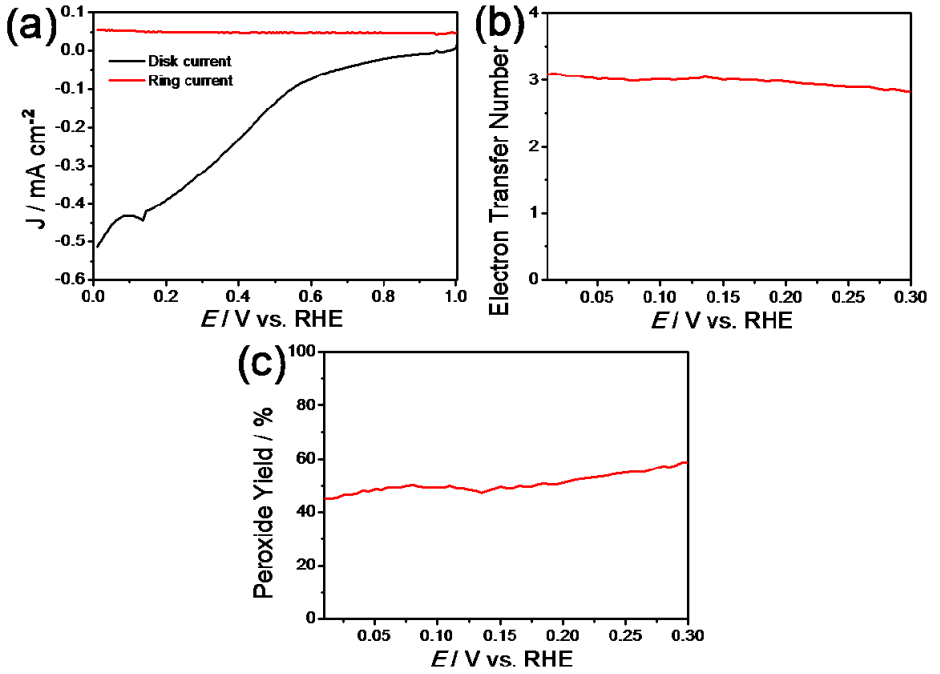


**Figure S5.** (a) RRDE voltammograms, (b) the *n* value and (c) $H_2O_2$ yield of C-1000 in $O_2$-saturated 0.5 M $H_2SO_4$.

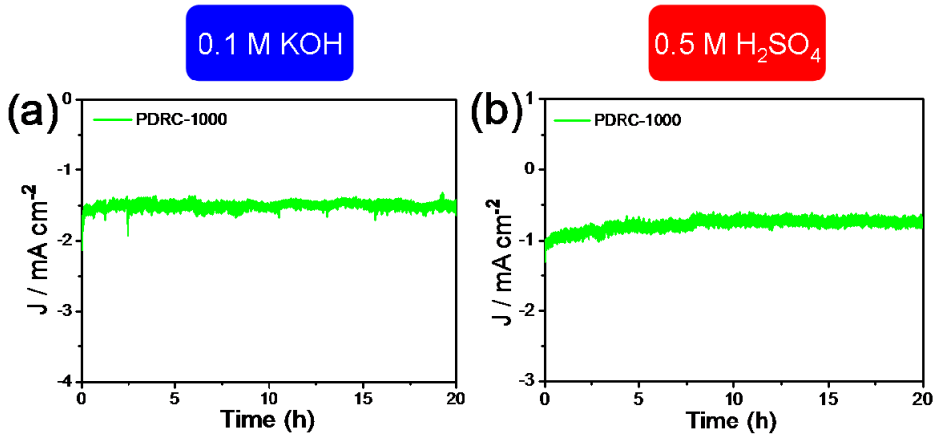


**Figure S6.** The stability measurements of PDRC-1000 electrode over 20 h in (a) alkaline and (b) acidic media, respectively.

**Table S1.** The atomic % of C, O, N and Ca of samples from XPS data.

| Samples | C (at %) | O (at %) | N (at %) | Ca (at %) |
|---|---|---|---|---|
| PDRC-800 | 79.59 | 9.6 | 10.11 | 0.7 |
| PDRC-900 | 68.04 | 14.42 | 13.12 | 4.42 |
| PDRC-1000 | 79.21 | 7.69 | 11.82 | 1.28 |

**Table S2.** The atomic % of the different N-bond types from XPS data.

| Samples | Pyridinic N (at %) | Pyrrolic N (at %) | Graphitic N (at %) |
|---|---|---|---|

| | | | |
|---|---|---|---|
| PDRC-800 | 4.21 | 3.65 | 2.25 |
| PDRC-900 | 6.41 | 5.70 | 1.01 |
| PDRC-1000 | 5.49 | 4.68 | 1.65 |

**Table S3.** The summary table of the samples used and their main properties.

| Samples | Treatment | BET surface area ($m^2$ $g^{-1}$) | Content of N (at %) |
|---|---|---|---|
| C-1000 | Ar, 1000 °C | 620 | 0 |
| PDRC-800 | $NH_3$, 800 °C | 809 | 10.11 |
| PDRC-900 | $NH_3$, 900 °C | 1034 | 13.12 |
| PDRC-1000 | $NH_3$, 1000 °C | 1158 | 11.82 |

## References

1. Yang, Y.; Lun, Z.; Xia, G.; Zheng, F.; He, M.; Chen, Q. Non-Precious Alloy Encapsulated in Nitrogen-Doped Graphene Layers Derived from MOFs as an Active and Durable Hydrogen Evolution Reaction Catalyst. *Energ. Environ. Sci* **2015,** *8*, 3563-3571.
2. Ferrero, G. A.; Preuss, K.; Fuertes, A. B.; Sevilla, M.; Titirici, M. M. The Influence of Pore Size Distribution on the Oxygen Reduction Reaction Performance in Nitrogen Doped Carbon Microspheres. *Journal of Materials Chemistry A* **2016,** *4*, 2581-2589.
3. Li, D. J.; Maiti, U. N.; Lim, J.; Choi, D. S.; Lee, W. J.; Oh, Y.; Lee, G. Y.; Kim, S. O. Molybdenum Sulfide/N-Doped CNT Forest Hybrid Catalysts for High-Performance Hydrogen Evolution Reaction. *Nano Letters* **2014,** *14*, 1228-1233.